Available online at www.sciencedirect.com

jmr&t Journal of Materials Research and Technology

journal homepage: www.elsevier.com/locate/jmrt

Original Article

The inhibition tendencies of novel hydrazide derivatives on the corrosion behavior of mild steel in hydrochloric acid solution

Zeinab R. Farag [a,*], *Moustapha E. Moustapha* [b], *El Hassane Anouar* [b], *Ghada M. Abd El-Hafeez* [a]

[a] *Faculty of Science, Chemistry Department, Fayoum University, 63514, Fayoum, Egypt*
[b] *Department of Chemistry, College of Science and Humanities in Al-Kharj, Prince Sattam Bin Abdulaziz University, 11942, Al-Kharj, Saudi Arabia*

ARTICLE INFO

Article history:
Received 21 September 2021
Accepted 9 December 2021
Available online 21 December 2021

Keywords:
Hydrazide derivatives
Polymer
Cyclic voltammograms
Mild steel
Corrosion inhibition

ABSTRACT

Three different simple and polymeric hydrazide derivatives have been synthesized, evaluated and investigated as corrosion inhibitors for mild steel in 1 M hydrochloric acid medium. The corrosion inhibition performance of these additives was evaluated using electrochemical impedance spectroscopy (EIS) and polarizations measurements. The inhibition efficiency obtained from polarization measurement followed the order of PACAH > ACAH > CAH. The inhibition efficiency of the polyhydrazide derivative (PACAH) at concentration of 50 and 500 ppm was found to be 90.66 and 96.79% respectively, while 500 ppm of cyanoacetohydrazide (CAH) was 39.79% and for the monomer N-acryloyl-N′-cyanoacetohydrazide (ACAH) was 88.66%.

The surface morphology of the steel electrode was studied with and without the inhibitor after immersion in 1 M HCl solution for 6 h using SEM, EDAX and AFM measurements. The results showed an improvement in the surface morphology where the flawed regions were repaired and the cracks were healed. This improvement was attributed to the adsorption of the inhibitor molecules and the formation of a protective layer at the steel surface. The adsorption isotherm indicated a spontaneous physical adsorption of the inhibitor on the surface of mild steel electrode. Quantum chemical calculation was used to correlate the inhibition efficiencies data of the hydrazide derivatives with their electronic structural parameters. Theoretical calculations supported and elucidated the experimental results.

* Corresponding author.
E-mail address: zrf00@fayoum.edu.eg (Z.R. Farag).
https://doi.org/10.1016/j.jmrt.2021.12.035

1. Introduction

Mild steel is one of the widely used constructional materials and its corrosion behavior has been the concern of many researchers especially in acidic solutions. The aggressive effect of the acidic environment resulted in the dissolution of mild steel and this process could be retarded by the addition of suitable corrosion inhibitor. Because of their versatile characters the corrosion behavior of mild steel alloys have been studied in acidic corrosive media. Mineral acids, sulfuric acid and hydrochloric acid are commonly used in these evaluations [1–4].

To provide required control against corrosion a small amounts of corrosion inhibitors were added to the corrosive medium. Most of these inhibitors are organic in nature i.e. compounds contains oxygen, nitrogen and sulphur. These compounds adsorbed on the metal surface through these atoms [2,4].

Different heterocyclic compounds were synthesized by Khadom et al. [5] these compounds were then tested as corrosion inhibitors for mild steel in 0.5 M HCl and their inhibition efficiency exceeded 95%. Thiazole hydrochloride derivative was tested a as corrosion inhibitor of steel in acidic solution. Gravimetrical, electrochemical, surface morphology and theoretical simulation were measured to investigate the corrosion behavior. It was found that a spontaneous protective layer was formed and chemically adsorbed on the surface of steel results in an inhibition efficiency of 95% [6]. Also, the corrosion behavior of low carbon steel was examined using 1-[(5-Phenyl-1,3, 4-oxadiazol-2-yl)thio] acetone (POTA) [7] and some triazole derivatives [8]. The inhibition efficiency of these compounds was found to be more than 70 and 96% respectively, theoretical quantum chemical calculations was used to confirm the experimental results.

Nitrogen and sulphur containing organic compounds such as pyrazoline derivatives, benzimidazole, benzenesulfonamide and Schiff bases were also investigated. The inhibition occurs through adsorption of the inhibitor molecules on the metal surface [9–15].

One of the widely used organic compounds are hydrazide derivatives [16] which have been employed as potential inhibitors for controlling the corrosion process of mild steel. The influence of some organic acid hydrazides, such as the hydrazides of salicylic acid, anthranilic acid, benzoic acid and cinnamic acid on the corrosion behavior of mild steel in 1 N HCl was studied. The potentiodynamic polarization measurements indicated that all these hydrazides are mixed inhibitors except that's of salicylic acid [17]. Also, N-Phenyl oxalic dihydrazide and oxalic N-phenylhydrazide N′-phenylthiosemicarbazide were also used as inhibitors. The results reveals the higher performance of oxalic N-phenylhydrazide N′-phenylthiosemicarbazide on the corrosion behavior of mild steel in 1 M HCl solution [18].

The corrosion inhibition studies of coumarin derivatives on the corrosion behavior for mild steel in acidic medium were introduced by Zinad et al. [19] It was concluded that the tested coumarin derivative is an excellent corrosion inhibitor with high inhibition efficiency. The mechanism of adsorption was found to be a physical adsorption mechanism. Theoretical studies have shown that the entities in coumarin molecules were bonded to the metal surface through the nitrogen, sulfur and oxygen atoms.

In the view of environmental protection, the application of green effective inhibitors for metal corrosion is of great interest [20]. An example of the eco-friendly compounds is thiourea functionalized glucosamine derivatives namely 5-hydroxy-1-phenyl-4-(1,2,3,4-tetrahydroxybutyl)imidazolidine-2-thione (GA-1) and 1-phenyl-3-(2,4,5-trihydroxy-6-(hydroxymethyl)tetrahydro-2H-pyran-3-yl)thiourea (GA-2). The electrochemical tests and surface analyses indicate that both GA-1 and GA-2 have high inhibition performance and it was found to be 97.7% for GA-2 [21]. Also, Losartan potassium film for corrosion inhibition of mild steel in HCl medium [22]. The inhibition performance values increased to 88.9%, 91.8%, and 92.0% for 5 mM LP at 298, 308, and 318 K, respectively.

The corrosion inhibition effect of expired ampicillin and flucloxacillin drugs for mild steel in aqueous acidic medium was evaluated. The observed high inhibition efficiencies of the studied expired drugs may be due to the formation of protective layers on the steel surface as a result of the powerful adsorption of the drug species [23].

A hydrazide derivative namely 2-(2-hydrazinyl-1,6-dihydro-6-oxopyrimidin-4-yl) acetohydrazide was synthesized by Abdallah et al., this compound has been tested as a corrosion inhibitor for mild steel in both 1 M HCl and 0.5 M H_2SO_4 solutions, the inhibition efficiency in HCl was found to be higher than that in H_2SO_4 solution [24]. Arrouji and his coworkers synthesized pyrazole cyanohydrazides and the corrosion inhibition efficiency of these derivatives has been examined on steel in 1 M HCl, it was found that the efficiency of these inhibitors was increased with the increasing of the concentration of inhibitors and decrease upon rising temperature [25]. Recently, Chaouiki et al. studied the inhibition efficiency of two synthesized hydrazone derivatives on mild steel (MS) in 1.0 M HCl [26]. The inhibition performance was investigated using weight loss measurements, electrochemical techniques, and scanning electron microscope (SEM) coupled with energy-dispersive X-ray spectroscopy (EDAX). The used inhibitors presented maximum inhibition efficiencies of 96% and 84%. It was found that the used inhibitors affected both anodic and cathodic reactions (mixed inhibitors) and their adsorption was found to be a combination of chemisorption and physisorption, obeyed the Langmuir isotherm model. The inhibition effect of thiosemicarbazide of phenyl hydrazide of fatty acids on mild steel in acid solution was also investigated [27].

The influence of 2-(3, 4, 5-trimethoxybenzylidene) hydrazinecarbothioamide (TMBHC) as inhibitor was tested using Tafel polarization and electrochemical impedance spectroscopy (EIS). The results showed that the inhibition efficiency increased with increasing of both inhibitor concentration and temperature [28]. Hydrazone derivatives have been used as green inhibitors for mild steel in 1 M HCl. These compounds exhibited a high inhibition performance and it is increases with increasing their concentrations [26]. Novel pyridinium [29] and Imidazolium-derived polymeric ionic liquid [30] were also used as corrosion inhibitors for mild steel in 1 M HCl. The inhibition efficiency was of 88.8% for IPyr-C_2H_5 and 92.3% for IPyr-C_4H_9, and it was found to be

exceeded 96% in case of using of the Imidazolium-derived polymeric ionic liquid (PIL).

In this article, a new organic inhibitors either simple compounds or polymeric additive belong to hydrazide family were synthesized. Then these compounds were tested as corrosion inhibitors for mild steel in 1 M HCl solution. The corrosion inhibition performance of these compounds was evaluated using electrochemical impedance spectroscopy (EIS) and polarizations measurements.

2. Experimental

2.1. Materials and methods

N-cyanoacetohydrazide (CAH), acryloyl chloride and dimethyl formamide (DMF) were obtained from Sigma–Aldrich, Germany. Methanol, potassium persulphate, sodium bisulphite and hydrochloric acid from El-Gomhouria Company for trading drugs, chemicals and medical supplies, Egypt (used as received). Deionized water (DIW) was used for preparation of solutions.

2.2. Preparation of the hydrazide derivatives

The first compound N-cyanoacetohydrazide (CAH) was used as the starting material to prepare the monomer, N-acryloyl-N′-cyanoacetohydrazide (ACAH) according to the method stated in literature [31]. Later on 1 mol/L of ACAH in DIW was then polymerized using redox initiators (potassium persulphate and sodium bisulphite) of concentration equal to 5×10^{-2} mol/L at 55–60 °C in water-bath for 3 h. The precipitated polymer, poly (N-acryloyl-N′-cyanoacetohydrazide) (PACAH) was then filtered off, washed with DIW and dried. The intrinsic viscosity of PACAH was found to be 4.7 g/cm^3 using DMF [31,32].

2.3. Electrochemical measurements

The composition of the mild steel electrode was mentioned in Table 1. The electrode was prepared in the form of cylindrical rod and mounted into glass tubes of appropriate diameter by epoxy resin leaving a free surface area of 0.4 cm^2 to contact the solution. The steel electrode was polished mechanically before each measurement using consecutive emery papers up to 200 grit then rubbed by smooth polishing cloth. Later it was washed carefully with deionized water and rapidly transferred to the electrolytic cell. An electrochemical cell used for electrochemical measurements was a double jacket multi-necks 250 ml flask. It is a three electrode all glass cell with a platinum counter electrode and saturated Calomel electrode (SCE) as a reference electrode [33,34]. All measurements were carried out in stagnant, naturally aerated 1 M HCl aqueous solution free or containing different concentrations of CAH, ACAH or PACAH (see Fig. 1). The potentiodynamic polarization and impedance measurements were performed using an electrochemical workstation (Voltalab 10 PGZ "All-in-one" potentiostat/Galvanostat). The potentials were measured against and referred to the saturated calomel reference electrode ($E^\circ = 0.245$ V the standard hydrogen electrode (SHE)). The electrode potential was left in the electrolyte to achieve the steady state until the potential change did not exceed 0.1 mV min^{-1}. This potential was taken as the steady state potential, E_{ss}. The potentiodynamic experiments were conducted at a scan rate of 10 mV s^{-1}. The values of the corrosion potential, E_{corr}, and corrosion current density, i_{corr}, were extrapolated from the potentiodynamic polarization curves. For all EIS measurements, excitation amplitude of 10 mV peak-to-peak in the frequency range from 50 mHz to 100 kHz was used. The corrosion inhibition efficiency, and the degree of adsorption, was calculated from the values of the corrosion current densities (polarization measurements) and the charge transfer resistances (impedance measurements). Different adsorption isotherms were tested and the adsorption free energy for the fitted data was calculated. The experimental results were reproduced and each experiment was carried out at least twice where a good reproducibility was attained.

2.4. Characterization of the morphology of steel surface

i. Scanning electron microscope SEM (ZEISS Sigma 500 VP) coupled with X-Ray Diffraction EDAX technique at energy

Table 1 – The chemical composition (weight%) of the mild steel electrode.

Element	C	Si	Mn	S	P	Cu	Cr	Ni	Al	Fe
Analysis	0.34	0.26	0.93	0.02	0.04	0.01	0.01	0.02	0.01	balance

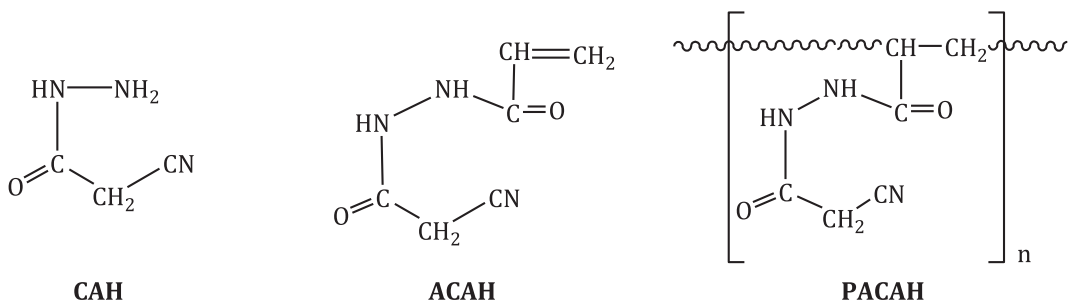

CAH **ACAH** **PACAH**

Fig. 1 – Chemical structure of the used hydrazide derivatives.

of 5.00 keV was used to study the morphology and characterize the microstructures of the polished, corroded and inhibited surfaces of the steel samples in HCl medium with and without inhibitor. X-ray diffraction patterns were collected using Cu-Ka monochromatic radiation at room temperature on a Bruker D8 ADVANCE diffractometer.

ii. Atomic Force Microscopy AFM and optical measurements

Atomic Force Microscopy (AFM) model (Nano-surf. Flex AFM version 5, for C3000 Control software version 3.6) was used to evaluate the topographical parameters of steel surface such as the morphology and roughness after immersion in 1 M HCl with and without the inhibitor.

2.5. *Computational details*

The ground states of CAH, ACAH and PACAH were optimized at the B3LYP/6-31G (d) level of theory as implemented in Gaussian software [35]. All optimized geometries were true minima were (Absence of imaginary frequencies). To determine the molecular and electronic properties that may have influence the corrosion inhibition of the synthesized monomer and its derivative a set of properties were calculated including the ionization potential (IP), electronic affinity (EA), gap energy between the HOMO and LUMO (ΔE), electronegativity (χ), chemical hardness (η), softness (S = 1/η), electrophilicity (ω) and dipole moment (μ)using the following formulae:

$$IP = -E_{HOMO} \tag{1}$$

$$EA = -E_{LUMO} \tag{2}$$

$$\chi = \frac{IP + EA}{2} \tag{3}$$

$$\eta = \frac{(IP - EA)}{2} \tag{4}$$

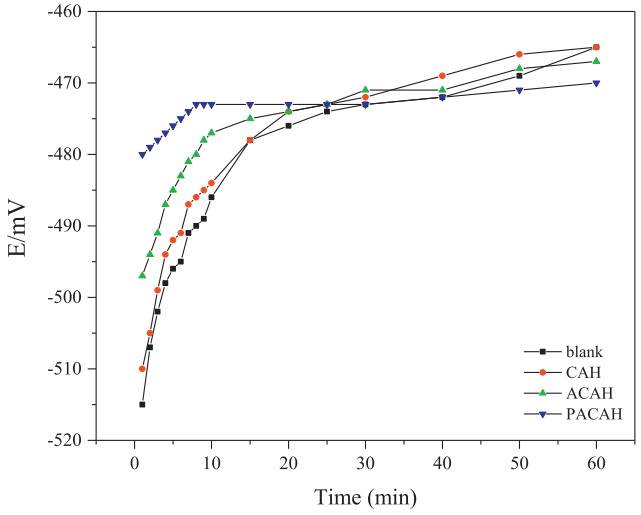

Fig. 2 – Variation of the open circuit potential of mild steel electrode with time in stagnant naturally aerated 1 M HCl solution containing 500 ppm of CAH, ACAH and PACAH at 25 °C.

$$S = \frac{1}{\eta} \tag{5}$$

$$\omega = \frac{\mu^2}{2\eta} \tag{6}$$

$$\mu = \sqrt{\mu'^2_x + \mu'^2_y + \mu'^2_z} \tag{7}$$

Further, the fraction of the transferred electrons (ΔN) between the inhibitor and interface of metal/solution was calculated through the Pearson theory [36] as in Equation (8):

$$\Delta N = \frac{\chi_{Fe} - \chi_{inh}}{2(\eta_{Fe} + \eta_{inh})} \tag{8}$$

where χ represents the electronegativity, Fe is the iron atom, η is the hardness and *inh* is for the inhibitor. In addition, the corrosion inhibition of these compounds may related to the nucleophilic and electrophilic sites that may bind to the interface of metal/solution. Thus, the electrostatic potential (ESP) and frontier molecular orbital (FMO) of CAH, ACAH and PACAH were determined at the same level of theory. In ESP maps, the red color indicates the negative region, which corresponds to hydrogen bond acceptors; while the blue color is an indication of the positive region, which corresponds to hydrogen bond donors. The solvation effects were taken into account implicitly by using the polarizable continuum model (PCM). In this model, the inhibitor is embedded into a cavity surrounded by solvent described by its dielectric constant ε (*e.g.*, for water ε = 78.3553) [37]. The ESPs and frontier molecular orbitals *HOMO* and *LUMO* were visualized using Gaussian View 6.

3. Results and discussion

3.1. *OCP measurements*

The OCP measurements of the mild steel electrode against SCE were recorded and tested for 60 min in stagnant naturally

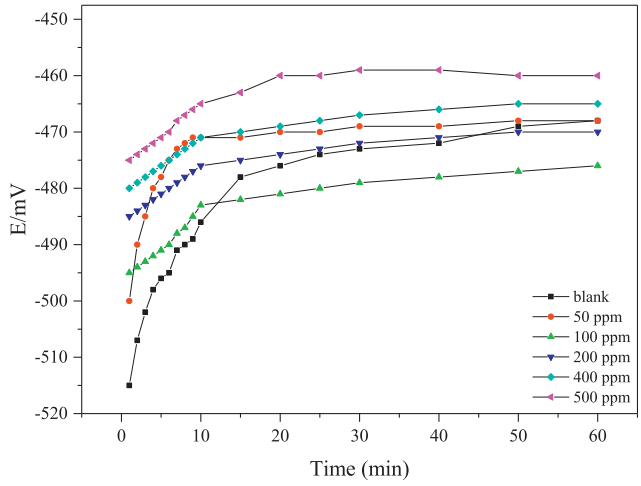

Fig. 3 – Variation of the open circuit potential of mild steel electrode with time in stagnant naturally aerated 1 M HCl aqueous solution containing different concentrations of PACAH at 25 °C.

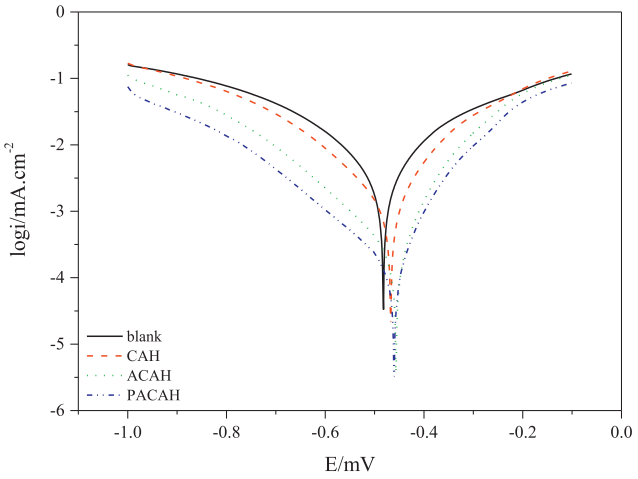

Fig. 4 – Potentiodynamic polarization curves for mild steel electrode after 60 min of electrode immersion in stagnant naturally aerated 1 M HCl solution containing 500 ppm of CAH, ACAH and PACAH at 25 °C.

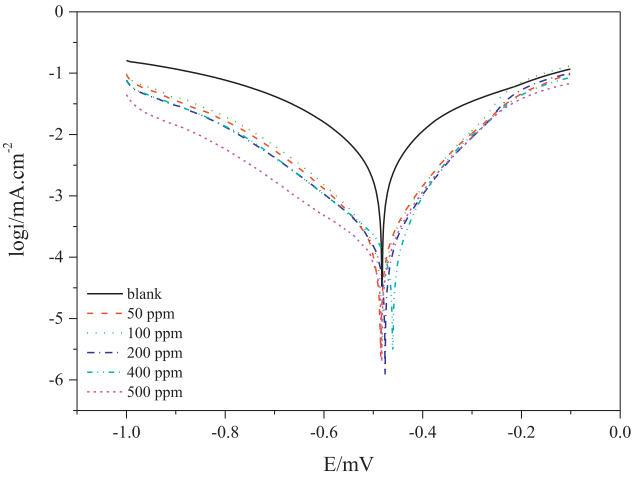

Fig. 5 – Potentiodynamic polarization curves for mild steel electrode after 60 min of electrode immersion in stagnant naturally aerated 1 M HCl solution containing different concentration of PACAH at 25 °C.

aerated solution of 1 M HCl (blank) and in the presence of 500 ppm of CAH, ACAH and the polymer PACAH at 25 °C using a high impedance auto-ranging multimeter (Keithley Model 130 A Germany) to record the individual test potentials. The Ess values were shifted to more positive potentials than that of the blank. This shift was related to the inhibition effect of the prepared materials. The value of Ess was always more positive than the immersion value (E_{oc} at t = 0), suggesting that a protective film may formed on the electrode surface. This result showed that the anodic rate reaction was decreased more than the cathodic reaction. For all additives, the OCP was found to reach a steady-state value within 30–40 min after electrode immersion in 1 M HCl solution, as showed in Fig. 2.

The open-circuit potentials (OCP) of mild steel in different concentrations of PACAH were traced over 60 min from the electrode immersion in 1 M HCl solution. The results of these measurements were presented in Fig. 3. Generally, the steady state potential was reached within the first 30 min of the electrode immersion in the test solution. The potential became more positive with time indicating development of a passive film on the electrode surface. The steady state potential shifted either in the negative or the positive direction in the presence of the polymer. The direction of potential shift depends on the electrode composition and the type of the inhibitor. The potential shift may be attributed to the adsorption of the inhibitor molecules on the active sites and/or the deposition of corrosion products on the electrode surface.

3.2. *PDP measurements*

The PDP measurements of mild steel electrode in stagnant naturally aerated aqueous solution of 1 M HCl and 500 ppm of the inhibitor at 25 °C were investigated. The PDP results were recorded after the electrode had reached Ess. The data obtained were presented in Fig. 4. All polarization curves for the used inhibitors were qualitatively similar and generally showed a decrease in the corrosion current density, i_{corr}, in the presence of CAH, ACAH and PACAH respectively. The Tafel extrapolation method applied to analyze the polarization curves and calculated the corrosion parameters, i.e. E_{corr}, i_{corr}, polarization resistance (Rp), βa, and βc, reported in Table 2. This table shows that, the polymerized hydrazide derivative PACAH increases the corrosion resistance of the mild steel electrode in the acidic solution if compared with the simple derivatives CAH and the monomer ACAH. In particular, PACAH polymer increased the corrosion resistance; moreover,

Table 2 – Potentiodynamic polarization parameters for mild steel electrode after 60 min of the electrode immersion in stagnant naturally aerated 1 M HCl aqueous solution containing 500 ppm of CAH, ACAH and PACAH at 25 °C.

	E_{corr}/ mV	I_{corr}/ mA.cm^{-2}	βa/ mV	βc/ mV	CR/ mm.Y^{-1}	η
Blank	−482.0	0.956	66.3	−77.3	11.09	–
CAH	−467.1	0.495	58.3	−85.6	5.74	48.24
ACAH	−456.1	0.085	49.0	−85.6	0.987	91.1
PACAH	−483.4	0.033	52.1	−91.9	0.381	96.57

Table 3 – Potentiodynamic polarization parameters for mild steel electrode after 60 min of the electrode immersion in stagnant naturally aerated 1 M HCl aqueous solution containing different concentrations of PACAH at 25 °C.

	E_{corr}/ mV	I_{corr}/ mA.cm^{-2}	βa/ mV	βc/ mV	CR/ mm.Y^{-1}	η
blank	−482.0	0.956	66.3	−77.3	11.09	–
50 ppm	−485.0	0.089	67.8	−87.0	1.04	90.66
100 ppm	−481.8	0.086	56.4	−80.2	0.996	91.02
200 ppm	−475.7	0.076	65.9	−93.4	0.884	92.03
400 ppm	−459.7	0.058	51.0	−93.8	0.669	93.97
500 ppm	−483.4	0.034	52.1	−91.9	0.381	96.57

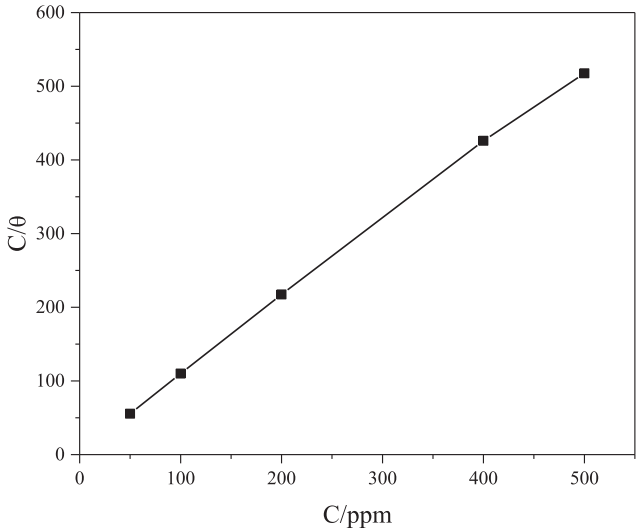

Fig. 6 – Adsorption isotherm of the adsorption of PACAH polymer on mild steel surface in naturally aerated stagnant aqueous solutions of 1M HCl containing different concentration of PACAH at 25 °C.

resulted in the lowest corrosion rate in acidic solution, as shown in Table 2, this observation can be explained by considering that the growth of a protective layer was enhanced on the mild steel electrode in the presence of PACAH polymer.

The effect of concentration of PACAH polymer on the surface of mild steel was investigated. Different concentrations ranging from 50 to 500 ppm have been used. Fig. 5 represented potentiodynamic polarization curves of these measurements. In general, the presence of different concentrations of PACAH in naturally aerated of 1 M HCl aqueous solution decreased the anodic and cathodic current density and had little effect on the corrosion potential as shown in Fig. 5. The results showed that PACAH retarded both the anodic and cathodic processes, i.e. PACAH acted as mixed inhibitor, where it is adsorbed on the electrode surface, blocking the active sites for the corrosion process, thus decreasing the exposed free electrode area to the corrosive medium [38].

The values of the corrosion parameters, corrosion current density, i_{corr}, corrosion potential, E_{corr}, and corrosion rate were calculated at different concentrations of polymer and were represented in Table 3. The results showed that there was irregular displacement in the corrosion potential, E_{corr}, values; this behavior was previously observed in many others studies [39]. In general, the corrosion current density decreased with increasing polymer concentration.

The corrosion inhibition efficiency (η) was calculated for the polymer inhibitor at different concentrations according to Equation (3.1). The values of η in all cases were also included in Table 3. The values of η showed that in most cases, the increase in polymer inhibitor concentration was accompanied by an increase in the corrosion inhibition efficiency. The inhibition efficiency of mild steel electrode reached its maximum values of 96.57% at 500 ppm.

$$\eta = [(i - i_{nh}) / i] \times 100 \quad (3.1)$$

Table 4 – Electronic and molecular properties of CAH, ACAH and PACAH calculated at in PCM model at the B3LYP/6-31G (d) level of theory.

	CAH	ACAH	PACAH
Ionization Potential (IP)	7.34	7.47	7.18
Electron Affinities (EA)	−0.37	1.39	1.16
Gap	7.71	6.08	6.02
X	3.48	4.43	4.17
H	3.86	3.04	3.01
S	0.13	0.16	0.17
Ω	1.57	3.23	2.89
ΔN	0.46	0.42	0.47
DM	10.07	11.23	6.38
Corrosion inhibition	39.79	88.66	96.79

3.3. *Mechanism of corrosion and inhibition*

In order to get a better understanding of the electrochemical process on the metal surface, adsorption characteristic were also studied for a corrosive media. This process was closely related to the adsorption of the inhibitor molecules and adsorption is known to depend on the chemical structure. The mechanism of adsorption was determined from the adsorption isotherm results and confirmed also by the quantum chemical calculations.

3.3.1. *The adsorption isotherm*

Adsorption isotherms are very important in determining the mechanism of organic electrochemical reactions. The adsorption of organic adsorbate on the surface of metal is regarded as substitutional adsorption process between the organic compounds in the aqueous phase $(org)_{aq}$. and the water molecules adsorbed on the metal surface $(H_2O)_{ads}$ according to the following process [40].

$$Org_{(sol)} + XH_2O_{(ads)} \leftrightarrow Org_{(ads)} + XH_2O_{(sol)} \quad (3.2)$$

where x represented the number of water molecules replaced by one molecule of organic adsorbate.

The adsorption of organic compounds can be described by two main mechanisms. Physical (electrostatic) adsorption required the presence of electrically charged metal surface and charged species in the bulk of the solution. The second was the chemisorption, which required charge sharing or charge transfer from the inhibitor molecule to the metal surface. In order to obtain more information about the nature of interaction between PACAH molecules and the electrode surface, different adsorption isotherms were investigated. The degree of surface coverage (θ) at different concentrations of the polymer in 1 M HCl aqueous solution was calculated from the corresponding electrochemical polarization measurements according to the equation below: [41].

$$\theta = (i_{corr} - i_{corr(inh)}) / i_{corr} \quad (3.3)$$

The obtained values of θ were fitted to different isotherms including Langmuir, Frumkin, and Temkin etc. The Langmuir isotherm equation was verified for the PACAH polymer, which is based on the assumption that all adsorption sites are equivalent and that particle binding occurs independently from nearby sites being occupied or not [42].

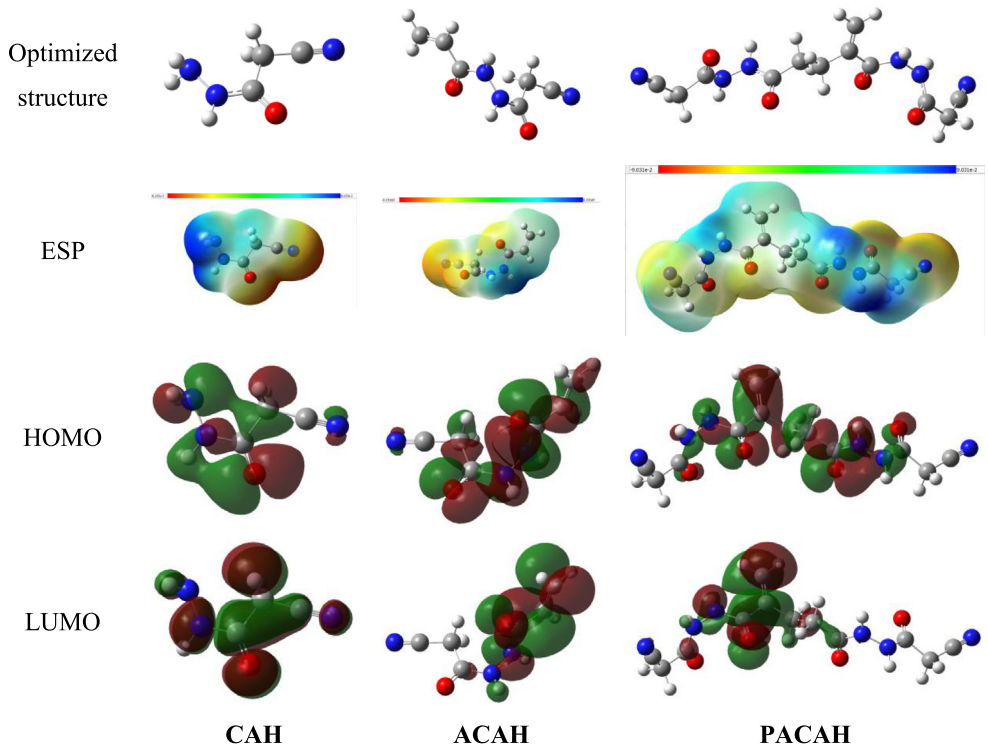

Fig. 7 – Optimized geometries, ESPs and frontier molecular orbitals of CAH, ACAH and PACAH.

$$KC = \theta/1-\theta \tag{3.4}$$

where C is the concentration of the inhibitor, θ, the fractional surface coverage and K is the adsorption equilibrium constant related to the free energy of adsorption, ΔG_{ads}, as [42,43]:

$$K = 1/Csolvent\exp(-\Delta G_{ads}/RT) \tag{3.5}$$

where, $C_{solvent}$ represents the concentration of the solvent, which is water i.e. 55.5 mol dm^{-3}, R is the universal gas constant (8.314 J $mol^{-1}K^{-1}$) and T is the absolute temperature [44,45]. The Langmuir adsorption isotherm can be rearranged to obtain the following mathematical formulation:

$$C/\theta = 1/K + C \tag{3.6}$$

So that a linear relationship can be obtained by plotting C/θ as a function of C, with a slope of unity. In Fig. 6 the proposed relation was plotted for the adsorption of PACAH on mild steel electrode in naturally aerated aqueous 1M HCl solution. The expected linear relationship was obtained and the free energy of adsorption, ΔG_{ads}, was calculated. A value of - 40 kJ/mol was usually adopted as a threshold value between chemisorption and physisorption [46]. The calculated values for the adsorption of the polymer inhibitor on the electrode surface is −5.057 kJ/mol which was less than −40 kJ/mol indicated a physical adsorption without chemical interaction between the polymer inhibitor molecules and the electrode surface. The low and negative value of ΔG_{ads} indicated a spontaneous adsorption of polymer inhibitor on the surface of mild steel electrode [47,48]. The possible mechanism of the adsorption of the inhibitor on the surface of mild steel electrode will be through the electron pair of N and O which blocked the mild steel surface and reduced the corrosive attraction of mild steel in HCl media.

3.3.2. *Computational results*

The above measurements revealed that the corrosion inhibition of the synthesized hydrazide derivatives increased with its length. CAH showed the lowest inhibition efficiency with 39.79% inhibition, the monomer ACAH showed lower inhibition than PACAH with inhibitions of 88.66% and 96.79%, respectively. In order to understand the observed results a set of molecular and electronic properties were calculated in water (Table 4). The calculated properties of CAH, ACAH and PACAH varied slightly from one to another. Hence, these properties may not be used as a stronger indicator of the increase of the inhibition. For all compounds, the calculated number of the transferred electrons from the inhibitor to the interface of metal/solution (ΔN) was positive values. This suggested that these compounds may have tendency to give the electrons to the interface of metal/solution. The optimized geometries, ESP and frontier molecular orbitals of CAH, ACAH and PACAH were represented in Fig. 7. From ESP charges and HOMO delocalization, one may relates the increase of inhibition efficiency to the increase of atomic sites (red region) donor of electrons and electronic delocalization in CAH, ACAH and PACAH. Indeed, PACAH shows the higher corrosion

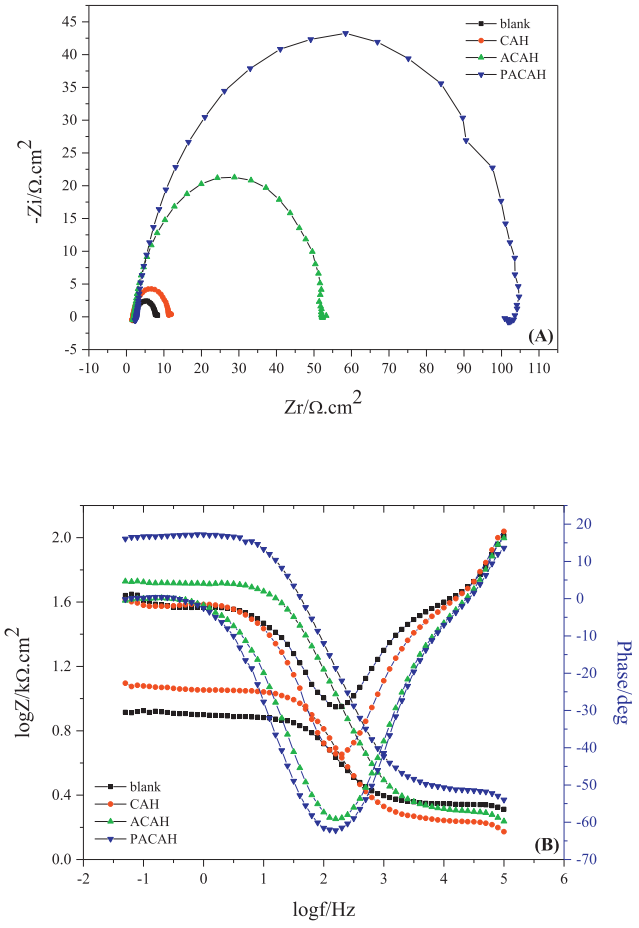

Fig. 8 – Impedance plots of mild steel electrode after 60min of electrode immersion in stagnant naturally aerated aqueous solutions of 1 M HCl containing 500 ppm of CAH, ACAH and PACAH at 25 °C, (A) Nyquist plots, (B) Bode plots.

inhibition, which is in accordance with the high number of red region, i.e., atomic site or functional groups donator of electrons. The data obtained from theoretical quantum chemical calculations provided good evidence to the experimental results obtained by EIS and polarization measurements.

3.4. *Electrochemical impedance measurements*

The results of the potentiodynamic polarization experiments were confirmed by EIS, which is a powerful technique in studying corrosion mechanisms and adsorption phenomena at the electrode/electrolyte interface. This study included the effect of CAH, ACAH and PACAH and the effect of different concentrations of PACAH on the corrosion behavior of mild steel electrode in 1M HCl solution.

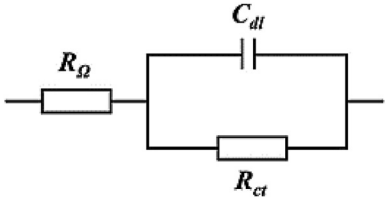

Fig. 9 – Equivalent circuit model for the analysis of the EIS data.

The Nyquist and Bode plots of mild steel electrode in 1M HCl and 500 ppm of CAH, ACAH and PACAH inhibitors were given in Fig. 8 A and B. It was observed that the electrode impedance increased remarkably in the presence of these inhibitors, indicating that the electrode surface became less active [49]. Also the phase maximum at the intermediate frequencies broadens, which suggests the presence of a protective layer (cf. Fig. 8B). The Nyquist spectrum (Fig. 8A) displayed an increased diameter of the semicircle, which reflected an increase in the R_{ct}.

An accurate analysis of impedance EIS data were fitted using a simple classical equivalent circuit model (*see* Fig. 9). The circuit consisting of a parallel combination between the electrode capacitance, Cdl, and the corrosion resistance, Rct, in series with a resistor, RΩ, representing the Ohmic drop in the electrolyte.

The calculated equivalent circuit parameters for mild steel after 60 min immersion in naturally aerated 1M HCl aqueous solution were displayed in Table 5. The results of these experiments showed that the charge transfer resistance, Rct, increased in the presence of CAH, ACAH and PACAH inhibitors. PACAH inhibitor recorded the higher Rct value for mild steel electrode.

The influence of the promising PACAH inhibitor concentrations on the corrosion process of mild steel electrode in 1M HCl aqueous solution was investigated using the electrochemical impedance spectroscopy. The Nyquist and Bode plots were presented in Fig. 10 (A and B). Bode plot showed one phase maximum at the intermediate frequency, the broadening of phase maximum increased in the presence for all concentrations, this means the presence of a progressive protective layer on the electrode surface.

Nyquist plot (Fig. 10A) showed an increase in the diameter of the impedance by increasing the polymer concentration, which depicted an increase in the inhibition resistance.

The impedance data were fitted to the simple equivalent circuit (c.f. 9) and the calculated data presented in Table 6. The inhibition efficiency was calculated according to the equation:

$$\eta = \left[\left((R_{ct})_{inh} - R_{ct}\right) / (R_{ct})_{inh}\right] \times 100 \quad (3.7)$$

The table highlighted an inverse relationship between Rct and the corrosion rate, implying that the increasing of PACAH inhibitor decreased the corrosion rate (increased the polarization resistance); in particular, the highest value of Rct were obtained for 500 ppm. In addition, an Rct increase was accompanied by a decrease in Cdl only, confirming that the investigated polymer can form a stable protective film on mild steel electrode. This result is in good agreement with the results of the potentiodynamic experiments.

3.5. *Surface morphology*

3.5.1. *SEM and EDAX measurements*

In order to identify the distribution and nature of microstructures that influence corrosion and inhibition behavior, a microstructural study was conducted on the different specimens. The profile images of virgin steel surface before and after contacting the solution was investigated by performing SEM

Table 5 – Equivalent circuit parameters for mild steel electrode after 60min of the electrode immersion in stagnant naturally aerated 1M HCl solution containing 500 ppm of CAH, ACAH and PACAH at 25 °C.

	$R_\Omega/\Omega.cm^2$	$Rct/\Omega.cm^2$	$Cdl/\mu F.cm^{-2}$	α	η/%
blank	2.21	5.81	346.0	0.994	–
CAH	1.73	9.65	260.5	0.993	39.79
ACAH	1.99	51.24	124.2	1	88.66
PACAH	3.28	181.2	138.7	0.996	96.79

and EDAX measurements after 60min immersion of the samples in 1M HCl aqueous solution at 25 °C in absence and in the presence of PACAH inhibitor. The SEM images represented in Fig. 11A showed the smooth surface of mechanically polished mild steel. The micrographs obtained for the mild steel after 60min immersion in 1M HCl aqueous solutions containing 500 ppm of PACAH inhibitor show an improvement in the surface morphology where the flawed regions were repaired and the cracks were healed as shown in Fig. 11C if compared with the uninhibited steel sample (Fig. 11 B).

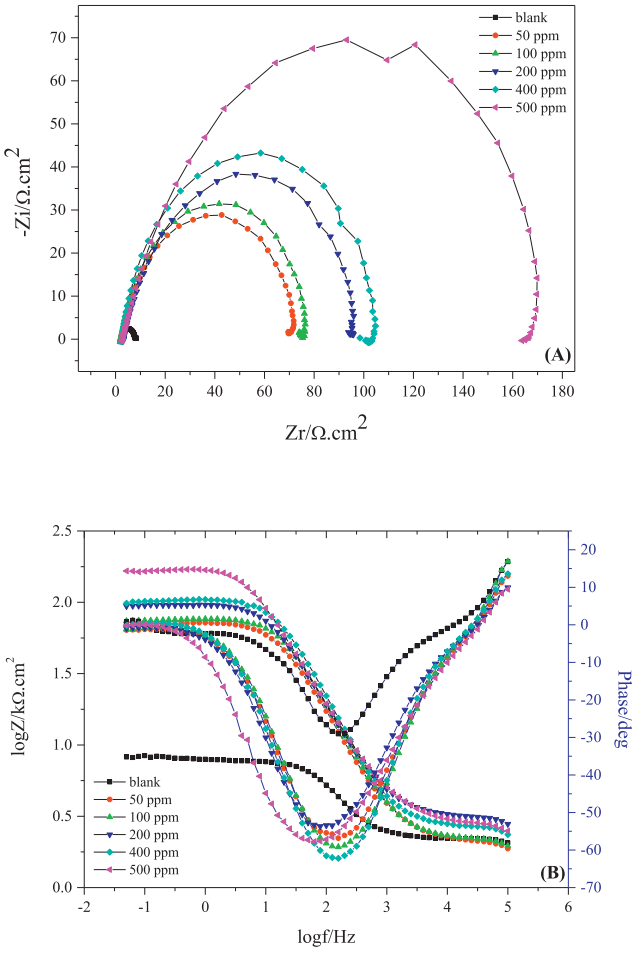

Fig. 10 – Impedance plots of mild steel electrode after 60min of electrode immersion in stagnant naturally aerated aqueous solutions of 1M HCl containing different concentrations of PACAH at 25 °C, (A) Nyquist plots, (B) Bode plots.

The results showed that in acidic solution without inhibitor, the surface was highly corroded and contained internal corrosion damage. However, in the presence of PACAH inhibitor there was an organic protective layer of PACAH developed on the electrode surface (Fig. 11C), which allowed a high degree of inhibition resistance, i.e. the surface morphology was highly protected due to the adsorption of PACAH and the corrosion of steel was significantly reduced.

Furthermore, EDAX analysis was performed to identify the elemental composition of the samples with and without the addition of inhibitor, after 1h immersion of the sample in 1M HCl aqueous solution at 25 °C the uninhibited solution contains a large percentage of O and Cl atoms, the oxygen content increased, which reflected the highest oxygen content (and therefore, the highest surface roughness and corrosion pitting) on the surface of the iron matrix. Whereas in the solution containing PACAH inhibitor, it was observed that the peaks corresponding to Cl and O were significantly reduced with the development of a new peak of N, which confirmed the adsorption of PACAH on the steel surface forming a protective layer, and this confirmed the increased efficiency of protection in presence of PACAH.

3.5.2. *Atomic force microscopy (AFM) analysis*

The surface profiles of untreated mild steel before and after immersion for 6h in 1M HCl solution with and without the inhibitor were represented in Fig. 12.

After immersion in an uninhibited aqueous HCl solution, the steel showed a rough texture surface indicating corrosion process as a result of the dissolution of the metal. The maximum roughness of the surface after immersion was ~183 nm (Fig. 12A). The topography and corresponding profile change of the steel surface immersed in the aqueous acidic solution containing 500 ppm of PACAH was represented in Fig. 12B. After immersion in the inhibited solution, the roughness of the surface was highly reduced indicating minimal metal dissolution due to protection of the surface by the inhibitor. The maximum roughness of the surface indicated by the profilometry after immersion was ~42 nm.

The figure of the surface topography showed that the corroded unprotected surface was quite different when compared with the protected one. The difference can be ascribed to polymeric additive PACAH in the test solution spontaneously adsorbed and formed a protective film layer at the steel surface.

Table 6 – Equivalent circuit parameters for mild steel electrode after 60 min of the electrode immersion in stagnant naturally aerated 1M HCl solution containing different concentrations of PACAH at 25 °C.

	$R_\Omega(\Omega.cm^2)$	R_{ct} $(\Omega.cm^2)$	Cdl $(\mu F/cm^2)$	α	η
Blank	2.21	5.81	346.0	0.994	–
50 ppm	2.36	71.01	112.0	0.996	91.8
100 ppm	1.81	79.19	127.0	0.997	92.7
200 ppm	3.39	97.15	103.5	0.996	94.0
400 ppm	2.73	103.3	97.30	0.997	94.4
500 ppm	3.28	181.2	138.7	0.996	96.7

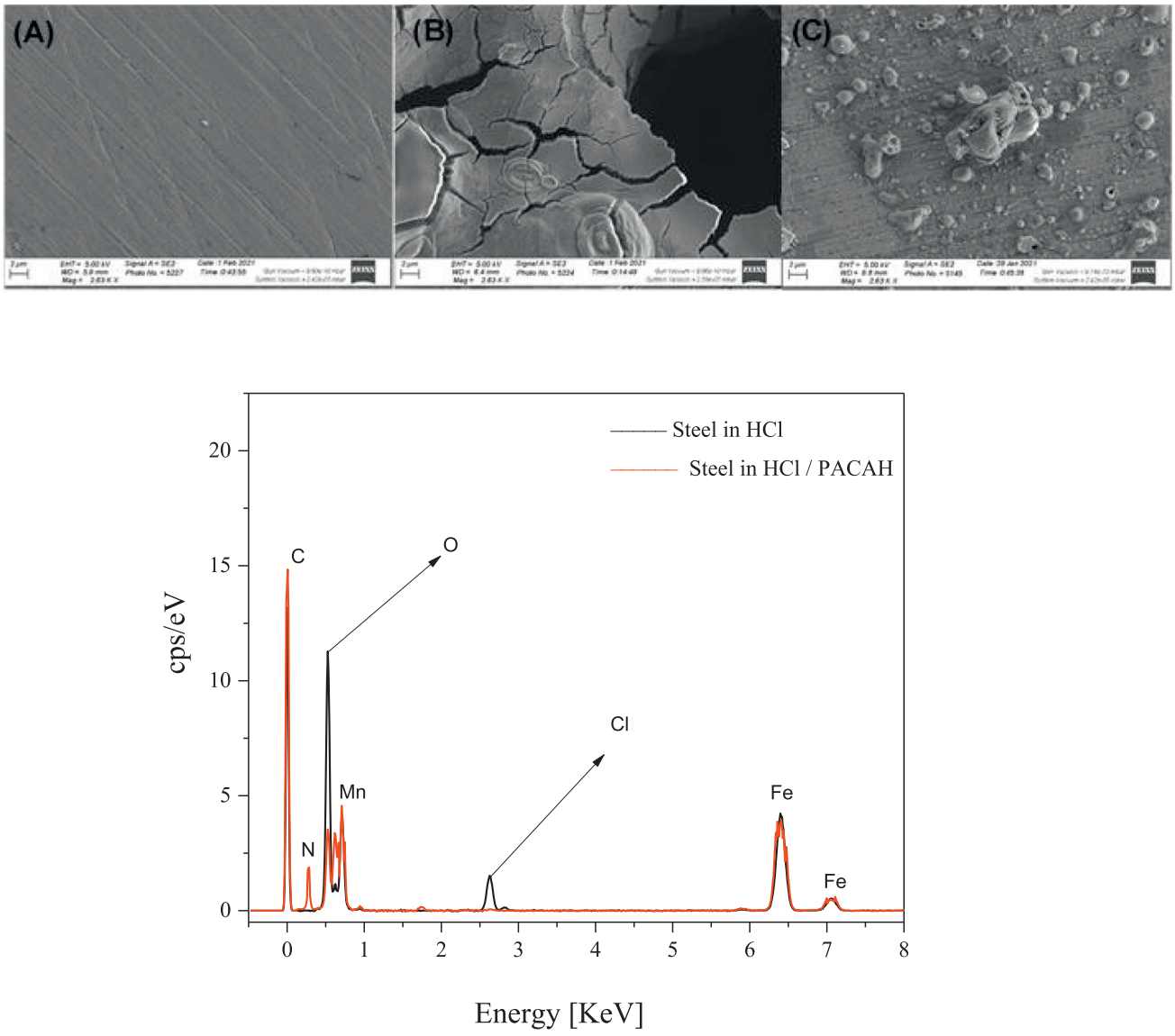

Fig. 11 – SEM and EDAX measurements of (A) the surface of a polished untreated mild steel electrode before contacting the solution and after immersion in (B) 1M HCl and (C) 1M HCl in the presence of 500 ppm of PACAH.

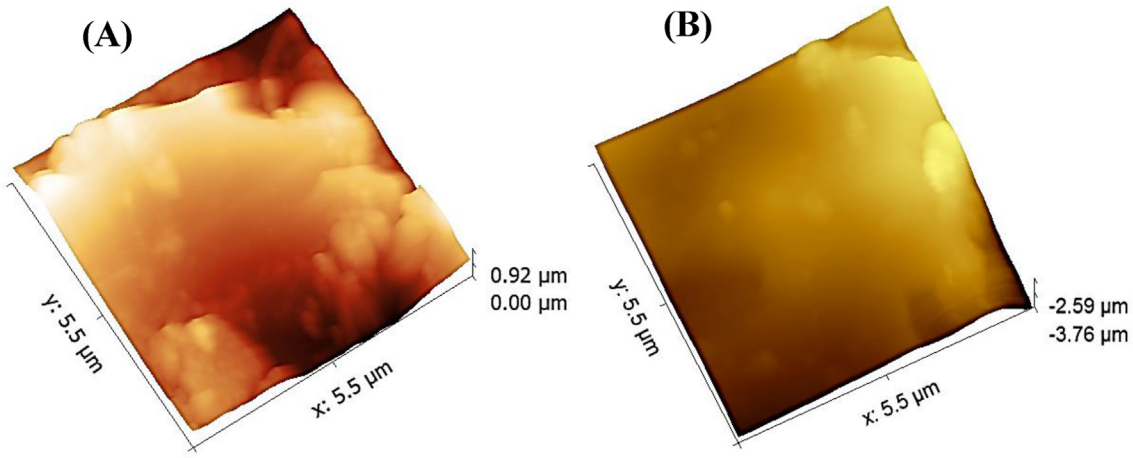

Fig. 12 – AFM topography of steel immersed for 6h in (A) uninhibited 1M HCl solution, and in (B) 1M HCL solution containing 500 ppm of PACAH.

4. Conclusion

Hydrazide derivatives were prepared using an organic synthesis route and then were used as a corrosion inhibitor for mild steel corrosion in 1M HCl solution. The organic synthesis method involved a facial synthesis of novel simple and polymeric hydrazide derivatives. The results of corrosion behavior of mild steel indicated that the hydrazide derivatives were found to be a potential acid corrosion inhibitors of mild steel in 1M hydrochloric acid media. The inhibition efficiency obtained from polarization measurement followed the order of PACAH > ACAH > CAH. The inhibition efficiency of lower concentrations of PACAH (50 ppm) was found to be 90.66% which is higher than that is for 500 ppm of CAH (39.79%) and the monomer ACAH (88.66%).

In other words, all of the three hydrazide derivatives inhibited corrosion by adsorption mechanism and the hydrazide polymer PACAH exhibited the better inhibition efficiency even when it was used at lower concentrations if it was compared with CAH and the monomer ACAH.

The SEM, EDX and FTIR analysis of inhibited mild steel specimen surface confirmed the formation of a protective film of the inhibitor molecules on steel surface. The results proved that the surface of the steel electrode was highly protected where the flawed regions were repaired and the cracks were healed.

The adsorption isotherm measurements indicated a spontaneous physical adsorption of the inhibitor on the surface of mild steel electrode. A good agreement was obtained between the calculated theoretical parameters and the experimental data, which determined the inhibition efficiencies for corrosion process of the hydrazide additives.

The hydrazide polymer PACAH has shown inhibition efficiency greater than 90%, which may be suitable for the industrial applications.

Declaration of Competing Interest

We confirm that there are no known conflicts of interest associated with the publication entitled **"The inhibition tendencies of novel hydrazide derivatives on the corrosion behavior of mild steel in hydrochloric acid solution"** and there has been no significant reason that could have influenced the manuscript outcome.

Acknowledgement

The authors extend their appreciation to the Deputyship for Research & Innovation, Ministry of Education in Saudi Arabia for funding this research work through the project number **2020/01/13175.**

REFERENCES

[1] Abd El-Hafeez GM, El-Rabeie MM, Gaber AF, Farag ZR. Tailored polymer coatings as corrosion inhibitor for mild steel in acid medium Journal of Coatings Technology and Research. 2021. p. 1–10. https://doi.org/10.1007/s11998-020-00426-0.

[2] Chakravarthy M, Mohana K. Inhibition behaviour of some isonicotinic acid hydrazides on the corrosion of mild steel in hydrochloric acid solution. International Journal of Corrosion 2013. https://doi.org/10.1155/2013/854781. 2013.

[3] Sayed AR, Abd El-lateef HM, Mohamad ADM. Polyhydrazide incorporated with thiadiazole moiety as novel and effective corrosion inhibitor for C-steel in pickling solutions of HCl and H 2 SO 4. Macromol Res 2018;26(10):882–91. https://doi.org/10.1007/s13233-018-6124-y.

[4] Tsoeunyane M, Makhatha M, Arotiba O. Corrosion inhibition of mild steel by poly (butylene succinate)-L-histidine extended with 1, 6-diisocynatohexane polymer composite in 1M HCl. International journal of corrosion 2019:1–13. https://doi.org/10.1155/2019/7406409. 2019.

[5] Ahmed SK, Ali WB, Khadom AA. Synthesis and investigations of heterocyclic compounds as corrosion inhibitors for mild steel in hydrochloric acid. Int J Integrated Care 2019;10(2):159–73. https://doi.org/10.1007/s40090-019-0181-8.

[6] Fadhil AA, Khadom AA, Liu H, Fu C, Wang J, Fadhil NA, et al. (S)6Phenyl2, 3, 5, 6tetrahydroimidazo [2, 1b] thiazole hydrochloride as corrosion inhibitor of steel in acidic solution: gravimetrical, electrochemical, surface morphology and theoretical simulation. J Mol Liq 2019;276:503–18. https://doi.org/10.1016/j.molliq.2018.12.015.

[7] Mahood HB, Sayer AH, Mekky AH, Khadom AA. Performance of synthesized acetone based inhibitor on low carbon steel corrosion in 1M HCl solution. Chemistry Africa 2020;3(1):263–76. https://doi.org/10.1007/s42250-019-00104-8.

[8] Ahmed SK, Ali WB, Khadom AA. Synthesis and characterization of new triazole derivatives as corrosion inhibitors of carbon steel in acidic medium. Journal of Bio- and Tribo-Corrosion 2019;5(1):1–17. https://doi.org/10.1007/s40735-018-0209-1.

[9] Abuelela AM, Bedair MA, Zoghaib WM, Wilson LD, Mohamed TA. Molecular structure and mild steel/HCl corrosion inhibition of 4, 5-Dicyanoimidazole: vibrational, electrochemical and quantum mechanical calculations. J Mol Struct 2021;1230:129647. https://doi.org/10.1016/j.molstruc.2020.129647.

[10] Al-Amiery A, Shaker L, Kadhum A, Takriff M. Corrosion inhibition of mild steel in strong acid environment by 4-((5, 5-dimethyl-3-oxocyclohex-1-en-1-yl) amino) benzenesulfonamide. Tribology in industry 2020;42(1). https://doi.org/10.24874/ti.2020.42.01.09.

[11] Caldona EB, Zhang M, Liang G, Hollis TK, Webster CE, Smith Jr DW, et al. Corrosion inhibition of mild steel in acidic medium by simple azole-based aromatic compounds. J Electroanal Chem 2021;880:114858. https://doi.org/10.1016/j.jelechem.2020.114858.

[12] Chaouiki A, Chafiq M, Rbaa M, Salghi R, Lakhrissi B, Ali IH, et al. Comprehensive assessment of corrosion inhibition mechanisms of novel benzimidazole compounds for mild steel in HCl: an experimental and theoretical investigation. J

Mol Liq 2020;320:114383. https://doi.org/10.1016/j.molliq.2020.114383.
[13] Lgaz H, Saha SK, Chaouiki A, Bhat KS, Salghi R, Banerjee P, et al. Exploring the potential role of pyrazoline derivatives in corrosion inhibition of mild steel in hydrochloric acid solution: insights from experimental and computational studies. Construct Build Mater 2020;233:117320. https://doi.org/10.1016/j.conbuildmat.2019.117320.
[14] Muthamma K, Kumari P, Lavanya M, Rao SA. Corrosion inhibition of mild steel in acidic media by N-[(3, 4-dimethoxyphenyl) methyleneamino]-4-hydroxy-benzamide. Journal of Bio-and Tribo-Corrosion 2021;7(1):1–19. https://doi.org/10.1007/s40735-020-00439-7.
[15] Shetty P. Schiff bases: an overview of their corrosion inhibition activity in acid media against mild steel. Chem Eng Commun 2020;207(7):985–1029. https://doi.org/10.1080/00986445.2019.1630387.
[16] Shetty P. Hydrazide derivatives: an overview of their inhibition activity against acid corrosion of mild steel. S Afr J Chem 2018;71:46–50. https://doi.org/10.17159/0379-4350/2018/v71a6.
[17] Quraishi M, Sardar R. D. Jamal and physics, Corrosion inhibition of mild steel in hydrochloric acid by some aromatic hydrazides. Mater Chem 2001;71(3):309–13. https://doi.org/10.1016/S0254-0584(01)00295-4.
[18] Larabi L, Harek Y, Benali O, Ghalem S. Hydrazide derivatives as corrosion inhibitors for mild steel in 1M HCl. Prog Org Coating 2005;54(3):256–62. https://doi.org/10.1016/j.porgcoat.2005.06.015.
[19] Zinad D, Jawad Q, Hussain M, Mahal A, Mohamed L, Al-Amiery A. Adsorption, temperature and corrosion inhibition studies of a coumarin derivatives corrosion inhibitor for mild steel in acidic medium: gravimetric and theoretical investigations. Int J Corros Scale Inhib 2020;9(1):134–51. https://doi.org/10.17675/2305-6894-2020-9-1-8.
[20] Boughoues Y, Benamira M, Messaadia L, Ribouh N. Adsorption and corrosion inhibition performance of some environmental friendly organic inhibitors for mild steel in HCl solution via experimental and theoretical study. Colloids Surf A Physicochem Eng Asp 2020;593:124610. https://doi.org/10.1016/j.colsurfa.2020.124610.
[21] Zhang Q, Hou B, Li Y, Zhu G, Liu H, Zhang G. Effective corrosion inhibition of mild steel by eco-friendly thiourea functionalized glucosamine derivatives in acidic solution. J Colloid Interface Sci 2021;585:355–67. https://doi.org/10.1016/j.jcis.2020.11.073.
[22] Qiang Y, Guo L, Li H, Lan X. Fabrication of environmentally friendly Losartan potassium film for corrosion inhibition of mild steel in HCl medium. Chem Eng J 2021;406:126863. https://doi.org/10.1016/j.cej.2020.126863.
[23] Alfakeer M, Abdallah M, Fawzy A. Corrosion inhibition effect of expired ampicillin and flucloxacillin drugs for mild steel in aqueous acidic medium. Int J Electrochem Sci 2020;15:3283–97. https://doi.org/10.20964/2020.04.09.
[24] Abdallah ZA, Ahmed MSM, Saleh M. Organic synthesis and inhibition action of novel hydrazide derivative for mild steel corrosion in acid solutions. Mater Chem Phys 2016;174:91–9. https://doi.org/10.1016/j.matchemphys.2016.02.055.
[25] El Arrouji S, Karrouchi K, Berisha A, Alaoui KI, Warad I, Rais Z, et al. New pyrazole derivatives as effective corrosion inhibitors on steel-electrolyte interface in 1M HCl: electrochemical, surface morphological (SEM) and computational analysis. Colloids Surf A Physicochem Eng Asp 2020;604:125325. https://doi.org/10.1016/j.colsurfa.2020.125325.
[26] Chaouiki A, Chafiq M, Lgaz H, Al-Hadeethi MR, Ali IH, Masroor S, et al. Green corrosion inhibition of mild steel by hydrazone derivatives in 1.0M HCl. Coatings 2020;10(7):640. https://doi.org/10.3390/coatings10070640.
[27] Toliwal S, Jadav K. Inhibition of corrosion of mild steel by phenyl thiosemicarbazides of nontraditional oils. J Sci Ind Res 2009;68(3):235–41. 0, http://nopr.niscair.res.in/handle/123456789/3161.
[28] Kumari PP, Shetty P, Rao AS. Electrochemical measurements for the corrosion inhibition of mild steel in 1 M hydrochloric acid by using an aromatic hydrazide derivative. Arab J Chem 2017;10(5):653–63. https://doi.org/10.1016/j.arabjc.2014.09.005.
[29] El-Hajjaji F, Ech-Chihbi E, Rezki N, Benhiba F, Taleb M, Chauhan DS, et al. Electrochemical and theoretical insights on the adsorption and corrosion inhibition of novel pyridinium-derived ionic liquids for mild steel in 1M HCl. J Mol Liq 2020;314:113737. https://doi.org/10.1016/j.molliq.2020.113737.
[30] Ardakani EK, Kowsari E, Ehsani A. Imidazolium-derived polymeric ionic liquid as a green inhibitor for corrosion inhibition of mild steel in 1.0M HCl: experimental and computational study. Colloids Surf A Physicochem Eng Asp 2020;586:124195. https://doi.org/10.1016/j.colsurfa.2019.124195.
[31] Mikhael MG. stability, Synthesis and thermal behaviour of poly (N-acryloyl, N′-cyanoacetohydrazide) and some of its metal complexes. Polymer degradation 1992;36(1):43–7. https://doi.org/10.1016/0141-3910(92)90046-8.
[32] Mohamed NA, Farag ZR, Sabaa MW. Thermal degradation behavior of poly (vinyl chloride) in presence of poly (N-acryloyl-N′-cyanoacetohydrazide). J Appl Polym Sci 2008;109(4):2362–8. https://doi.org/10.1002/app.27530.
[33] El-Rabiee M, Helal N, Abd El-Hafez GM, Badawy W. Corrosion control of vanadium in aqueous solutions by amino acids. J Alloys Compd 2008;459(1–2):466–71. https://doi.org/10.1016/j.jallcom.2007.04.293.
[34] Helal N, El-Rabiee M, Abd El-Hafez GM, Badawy W. Environmentally safe corrosion inhibition of Pb in aqueous solutions. J Alloys Compd 2008;456(1–2):372–8. https://doi.org/10.1016/j.jallcom.2007.02.087.
[35] Frisch MJ, Trucks GW, Schlegel HB, Scuseria GE, Robb MA, Cheeseman JR, et al. Gaussian 16 rev. C.01, city. 2016.
[36] Pearson RG. Hard and soft acids and bases. J Am Chem Soc 1963;85(22):3533–9. https://doi.org/10.1021/ja00905a001.
[37] Tomasi J, Mennucci B, Cammi R. Quantum mechanical continuum solvation models. Chem Rev 2005;105(8):2999–3094. https://doi.org/10.1021/cr9904009.
[38] Fuchs-Godec R. The adsorption, CMC determination and corrosion inhibition of some N-alkyl quaternary ammonium salts on carbon steel surface in 2 M H2SO4. Colloids Surf A Physicochem Eng Asp 2006;280(1–3):130–9. https://doi.org/10.1016/j.colsurfa.2006.01.046.
[39] Farooqi I, Quraishi M. Natural compounds as corrosion inhibitors for mild steel in industrial cooling systems. Eurocorrosion 1997;2:347.
[40] Bockris JOM, Reddy A. Modern electrochemistry. City: Plenum; 1976.
[41] Hladky K, Callow L, Dawson J. Corrosion rates from impedance measurements: an introduction. Corrosion J 1980;15(1):20–5. https://doi.org/10.1179/000705980798318627.
[42] Hitzig J, Titz J, Juettner K, Lorenz W, Schmidt E. Frequency response analysis of the Ag/Ag+ system: a partially active electrode approach. Electrochim Acta 1984;29(3):287–96. https://doi.org/10.1016/0013-4686(84)87064-4.
[43] Popova A, Sokolova E, Raicheva S. Relation between the molecular structure and protective action of organic inhibitors and their protective effect II. Inhibitors in acidic media *Khimia* Ind 1988;60:72–6.
[44] Chang S-H, Ryan M, Gupta R. B. Swiatkiewicz and surfaces, the adsorption of water-soluble polymers on mica, talc limestone,

various clay minerals. Colloids Surf A Physicochem Eng Asp 1991;59:59–70. https://doi.org/10.1016/0166-6622(91)80237-I.

[45] Vertel JJM, Vargas APV, García AV, Díaz DFM, Castelblanco AXR. Polymer adsorption isotherms with NaCl and CaCl2 on kaolinite substrates. Dyna: revista de la Facultad de Minas. Universidad Nacional de Colombia. Sede Medellín. 2019;86(210):66–73. https://doi.org/10.15446/dyna.v86n210.74361.

[46] Hajjaji N, Rico I, Srhiri A, Lattes A, Soufiaoui M, Ben Bachir A. Effect of N-alkylbetaines on the corrosion of iron in 1M HCl solution. Corrosion 1993;49(4):326–34. https://doi.org/10.5006/1.3316057.

[47] Elachouri M, Hajji M, Salem M, Kertit S, Aride J, Coudert R, et al. Some nonionic surfactants as inhibitors of the corrosion of iron in acid chloride solutions. Corrosion 1996;52(2):103–8. https://doi.org/10.5006/1.3292100.

[48] Savithri B, Mayanna S. Tetrabutyl ammonium iodide, cetyl pyridinium bromide and cetyl trimethyl ammonium bromide as corrosion inhibitors for mild steel in sulphuric acid. Indian J Chem Technol 1996;3:256–8.

[49] Badawy W, Elegamy S, Ismail KM. Comparative study of tantalum and titanium passive films by electrochemical impedance spectroscopy. Br Corrosion J 1993;28(2):133–6. https://doi.org/10.1179/bcj.1993.28.2.133.